Journal of Structural Geology, Vol. 6, No. 5, pp. 499 to 519, 1984
Printed in Great Britain

0191-8141/84 $03.00 + 0.00

A geometrical and kinematical approach to the nappe structure in an arcuate fold belt: the Cantabrian nappes (Hercynian chain, NW Spain)

M. JULIVERT and M. L. ARBOLEYA

Departamento de Geotectónica, Universidad Autónoma de Barcelona,
Bellaterra (Barcelona), Spain

(*Received* 26 *April* 1983; *accepted in revised form* 4 *November* 1983)

Abstract—In northwest Spain thrust sheets occur in an arcuate fold belt. The fault style consists of an array of thrusts, merging downdip into a single décollement surface. Most of the thrust sheets were initiated as thrusts cutting across flat lying beds. Folds above the hanging-wall ramps and some minor structures indicate that the body of the nappes has been subjected to an inhomogeneous simple shear parallel to bedding ($\gamma = 1.15$), with slip concentrated along bedding planes. This allows the rocks forming the nappe to remain unstrained. At the base of the nappes a thin zone of deformed rock exists. The thrust sheets die out laterally against an anticline–syncline couple, oblique to the thrust direction. A geometrical analysis shows that if anticline and syncline axes are oblique, the thrust sheet was emplaced with a rotational movement, which can be evaluated. As deformation progressed two sets of folds were formed: a circumferential set, following the arc, and a radial set. An arcuate trace of the thrust structures remains after unfolding the radial folds. With a rotational emplacement, the displacement vector for successive points has a progressively greater length, and forms a progressively lower angle with the thrust. The main thrust units are broken into several slices with rotational movements, so that each unit was curved as it was being emplaced, producing a first tightening of the arc. Later folding increased the arc curvature to its present shape. The palaeomagnetic data available support the above conclusions.

INTRODUCTION

DÉCOLLEMENT nappes are common structures in the frontal part of fold belts of different ages. The nappes of the Rocky Mountains, those of the Appalachian Valley-and-Ridge province or those in the Cantabrian zone (Iberian Peninsula), of the European Hercynian fold belt are well known examples of these kinds of structures.

In many respects, the nappes in the external part of different fold belts have similar characteristics, but in others they show important differences. Some of the nappes formed by a cover more or less attached to its basement are recumbent folds and exhibit strong internal folding (e.g. Morcles nappe, Helvetic Alps) and some others were emplaced as flat plates, bounded at the base by a thrust surface parallel to bedding, and lacking internal folding (e.g. Appalachian nappes, Valley-and-Ridge Province; Cantabrian nappes). Some are found in straight or very gently curved fold belts, while others occur in arcuate belts with a curvature which could increase during the progress of orogeny.

The aims of this paper are to define the geometry of décollement nappes in an arcuate fold belt such as the Hercynian belt in northwestern Spain, to consider the implications of the nappe emplacement, and to establish the tectonic evolution of the belt.

The generation of structures with an arcuate primary trace gives rise to space problems, especially if thrust sheets with important horizontal displacements occur along the arc. This is the case of the Cantabrian nappes, which seem to have been emplaced with a curved trace and a converging motion towards the centre of the arc. In order to establish a model for the Cantabrian nappes, the primary trace of the overthrusts must be elucidated, and to what extent the arc is primary or secondary, determined.

The nomenclature used in this paper is according to Butler (1982) and Boyer & Elliott (1982).

GEOLOGICAL SETTING

The décollement Cantabrian nappes occur in the frontal unmetamorphosed part (Cantabrian zone) of the Hercynian fold belt in NW Spain. This frontal part consists of a platform cover, formed by a varied succession of shallow-water terrigenous and carbonate formations, detached from its basement and split into many overthrust units. From their position in the foldbelt, as well as by their geometry, the Cantabrian nappes can be compared with the Rocky Mountains and with the Valley-and-Ridge nappes, in the Cordillerean and Appalachian fold belts. Nevertheless, a special character of the Cantabrian nappes not shown by these others is the pronounced arcuate shape of the belt.

The Hercynian fold belt crosses the Iberian Peninsula from southeast to northwest describing a well marked arc in the northwestern part of the Peninsula, extending into the Armorican massif, in France. The Cantabrian nappes occur in the core of this arc, facing roughly towards its centre and therefore giving the appearance of a converging movement.

The structure of the Cantabrian zone is the result of polyphase deformation. In this zone, décollement nappes coexist with folds of several generations. In broad terms, deformation started by the generation of décollement nappes with associated folds representing the structures into which the nappes die out along strike. The trace of these structures describes an arc, curving

through 180°. As deformation progressed, the tectonic style changed and the nappes began to fold flexurally. The nappes were at first folded more or less longitudinally by a set of folds which, together with the older structures, constitute the arc. Later, a radial fold set developed deforming both the nappes and the arcuate fold set. The radial set of folds fans out and vanishes westward showing that, at least during the last stages of its evolution, the arc tightened.

A description of the décollement units and an analysis of fold superimposition in the Cantabrian zone has been given in some previous papers (Julivert 1971a, Julivert & Marcos 1973). Figure 1 gives a structural sketch of the Cantabrian zone and the local names given to the different thrust units.

THE PROFILE OF THE CANTABRIAN NAPPES

Ramps and bedding thrusts in the Cantabrian nappes

The several Cantabrian nappes and thrust sheets although differing considerably in size, show identical characteristics. They were emplaced as plates of more or less flat-lying sediments which detached along a fault subparallel to the bedding and coinciding or nearly coinciding with the base of the Láncara Formation (limestones or dolostones, Early to Middle Cambrian in age). Each thrust unit forms a plate bounded at the base by a thrust surface consisting of bedding faults and ramps, and on top partly by the free surface and partly by the next overriding plate. In general, the plates show no internal folding contemporaneous with their emplacement; the few exceptional folds found occur in peculiar positions within the nappe.

Many of the Cantabrian nappes can be interpreted according to a two ramp model, although the ramps are seldom seen—the proximal due to burial and the distal due to pre-Mesozoic erosion. Because of erosion, the most superficial and frontal parts of the nappes are always lacking. One exception may be the Esla nappe, in the frontal part of which olistostromes related to its emplacement have been described (Arboleya 1981).

Considering only the pre-Westphalian part of the sequence, the sedimentary prism was wedge-shaped, thinning towards the core of the arc and thickening radially in the opposite direction. This shape is due mainly to the wedging out of the different Devonian and Silurian formations towards the core of the arc.

The configuration of thrust surfaces in the main thrust units and the position of the ramps and bedding faults inside the prism of sediments are shown in Fig. 2. The overall structure shown in this figure consists of an array of ramps and flats bifurcating and cutting up-sequence towards the core of the arc, merging downdip and affecting progressively deeper levels towards its margin.

Along the Narcea antiform there is a zone of deep faulting and these fault planes flatten when reaching the Palaeozoic sequence to merge with the bedding faults of the Cantabrian zone. This fault zone forms the boundary between an area where the Palaeozoic sequence has been stripped of the Pre-Cambrian (Cantabrian zone), with a thin-skinned type of tectonic structure without involving significant strain and without metamorphism, and an area (Westasturian–Leonese zone) with a fold structure involving Pre-Cambrian rocks and associated with the development of cleavage and metamorphism.

Ramp measurements

The overthrust surfaces follow the layering over large areas and the ramps are generally quite small. The best developed ramps are found in the Laviana and Rioseco thrust sheets and in the Rio Color tectonic window.

The Laviana and Rioseco thrust sheets have sinuous traces due to cross folding and subsequent erosion (Fig. 3). As both thrust sheets have suffered cross folding, in order to measure the ramps it is necessary first to unfold them, bringing one of the sheets into a horizontal position. For this purpose the precise shapes of La Foz and Felechosa cross synclines have been determined.

The La Foz syncline is a rather simple structure, with straight limbs, at the level of the Laviana thrust sheet, and with a somewhat box shape at the level of the Rioseco thrust sheet, the two hinges converging slightly westwards. The ramp between both units is exposed in the southern limb of the syncline. In the northern limb the trace of the ramp is also exposed, but below it, there is a small syncline related to the overthrusting. All these folds are open flexural folds, without associated cleavage or any significant strain. As the limbs of the folds are straight, the area can be subdivided into several regions (2 for the Laviana and 3 for the Rioseco sheet) in which the bedding has a statistically constant dip and strike (Fig. 4a). The results obtained by unrolling the cross folds and bringing the Rioseco sheet into a horizontal position are (Figs. 4b & c):

N15°E, for the direction of the bedding trace (L'') on the ramp, and consequently for the ramp direction,

N219°E, for the direction of the syncline axis below the foot-wall ramp, calculating its present orientation from the intersection of both limbs,

N223°E, plunging 14° to the S, for the same syncline, using field data and

22 to 33°, for the ramp dip.

The above results are reasonably consistent. The main arguments to support the validity of the results are as follows. (1) The bedding trace on the ramp and the axis of the fold in its foot-wall side, supposed to represent the ramp direction, are brought nearly to coincidence by unrolling the folds. The slight strike difference could be real and represent the curvature (primary or secondary) of the structures. (2) By rotating the two limbs of the syncline in the Laviana thrust sheet about the same rotation axis used to unroll the syncline in the Rioseco sheet, both limbs are brought nearly to coincidence, their strike and dip representing the strike and dip of the ramp. (3) The trace of the ramp in the southern limb of the syncline crosses the 'Mountain' Limestone (between

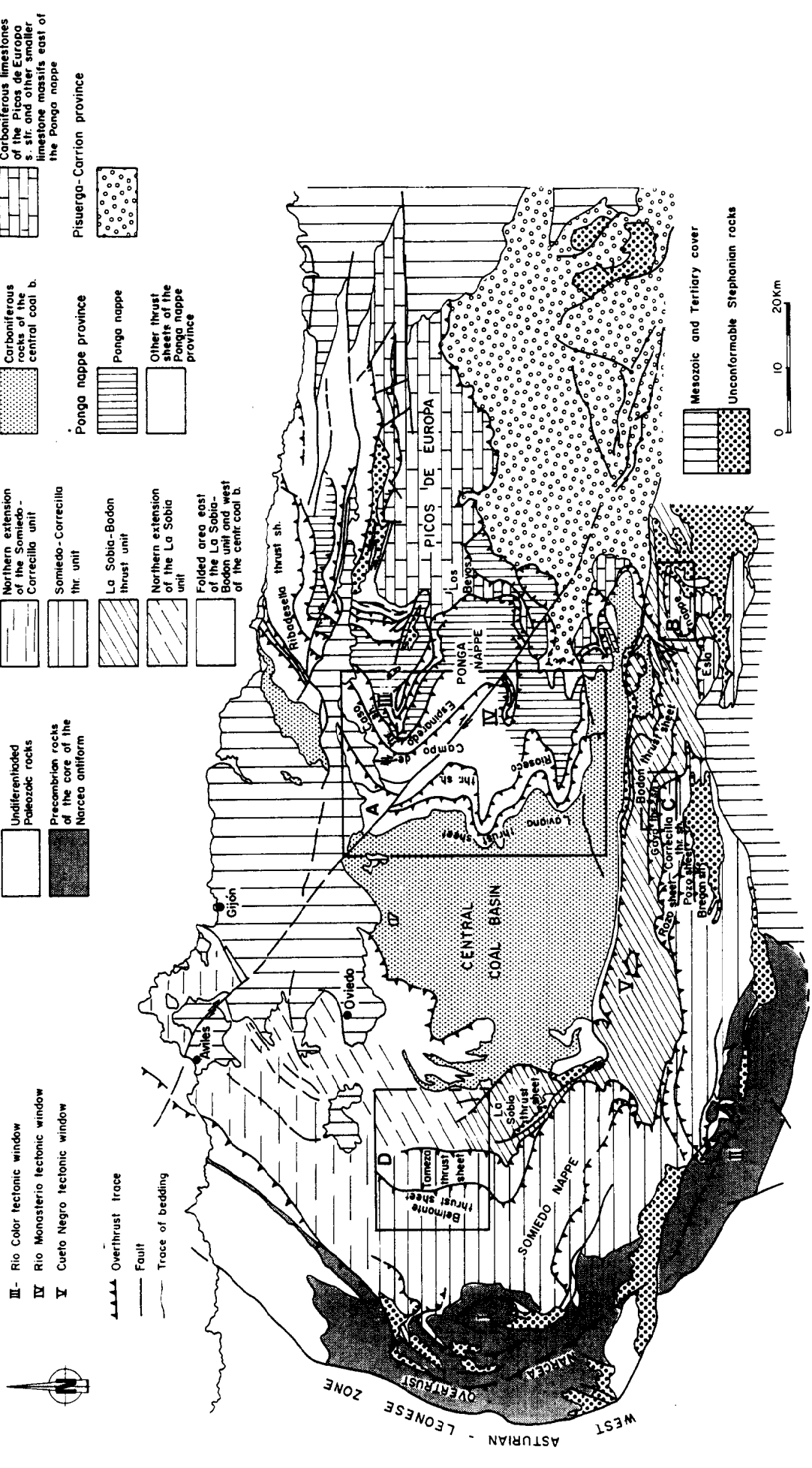

Fig. 1. Structural sketch of the Cantabrian zone. A, B, C, and D showing map areas represented in Figs. 3, 5 and 9.

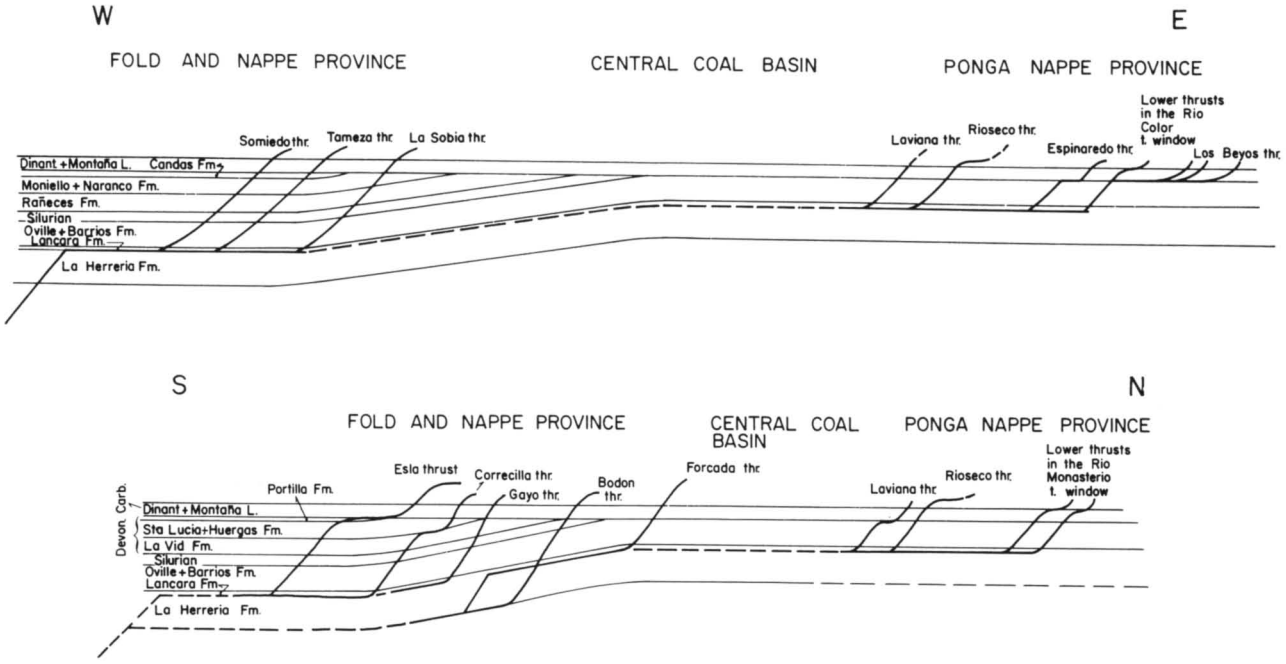

Fig. 2. Position of the thrust surfaces in the wedge of pre-Carboniferous sediments, for the main thrust units.

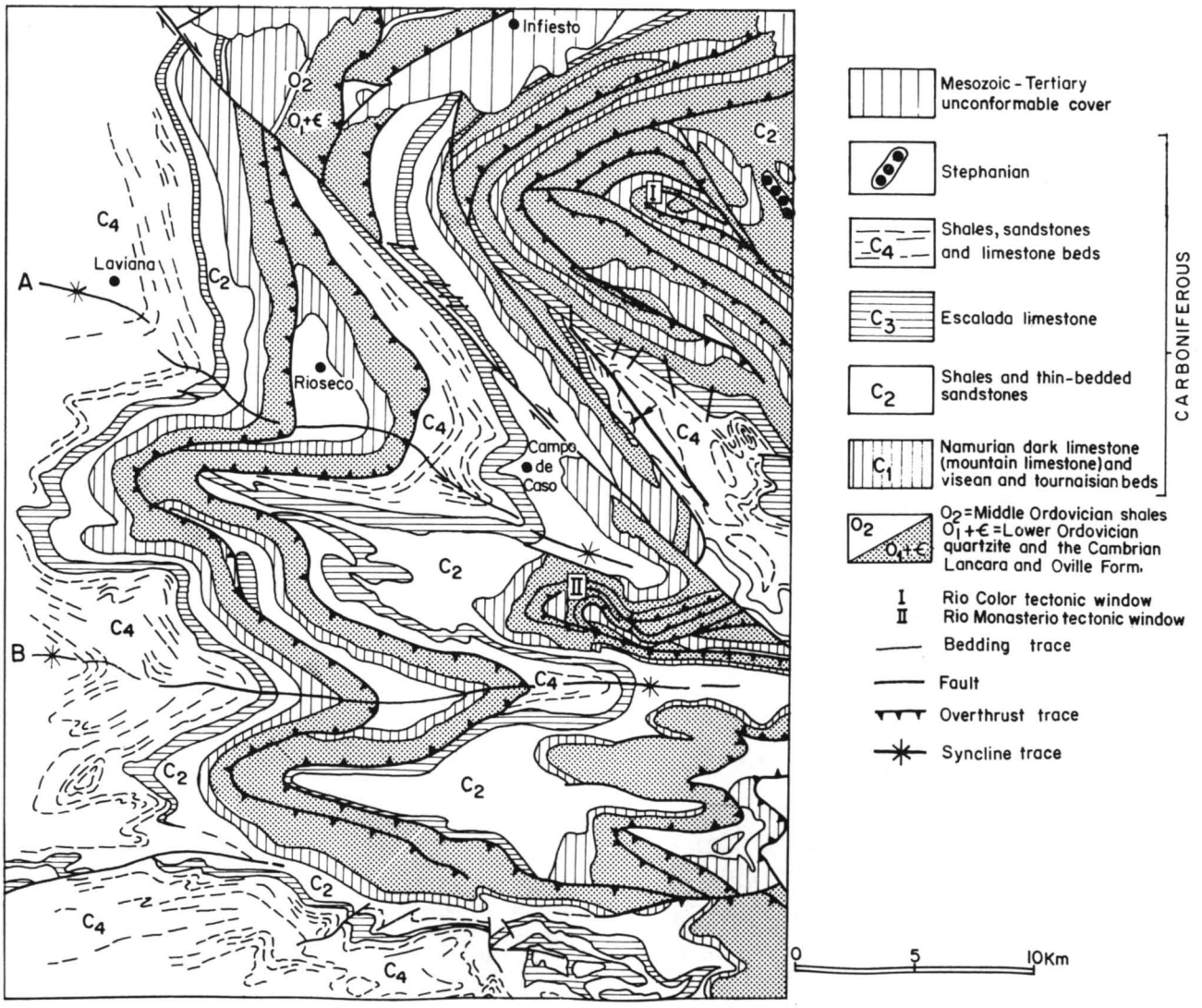

Fig. 3. Geological sketch map of the Laviana and Rioseco thrust sheets and western part of the Ponga nappe (area of the Rio Color and Rio Monasterio tectonic windows). (A) La Foz syncline. (B) Felechosa syncline. Map area labelled A in Fig. 1.

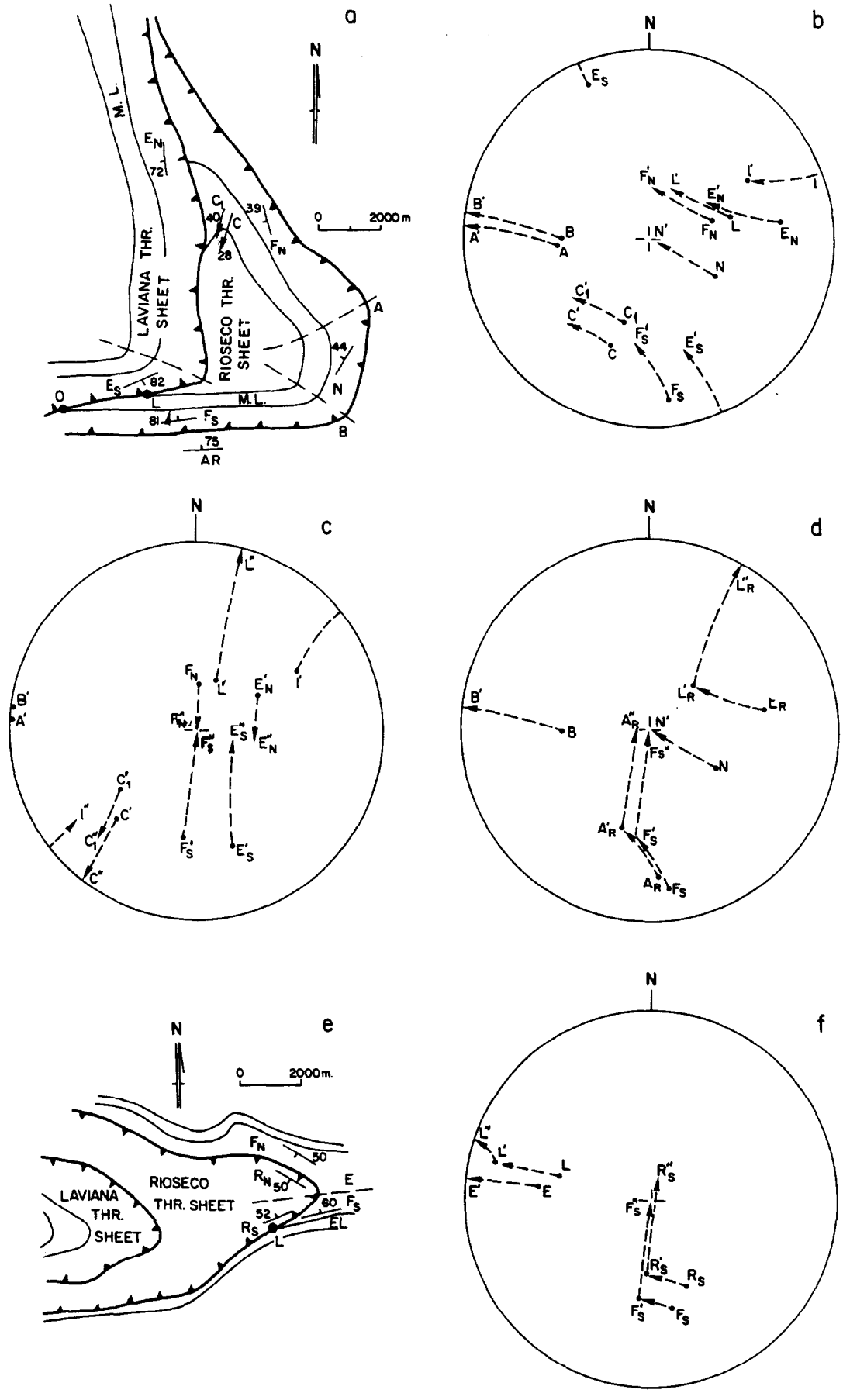

Fig. 4. Unfolding the Laviana and Rioseco thrust Sheets. (a) Field data (average values) in the La Foz syncline. F_N and F_S: dips of the fold limbs in the Rioseco thrust sheet. N, dip in the area between axes A and B. A and B, fold axes. C and C_1 axes of the fold below the foot-wall ramp calculated from the intersection of both limbs and directly measured in the field. En and Es, dips of the fold limbs in the Laviana thrust sheet. L, bedding trace of the Rioseco thrust sheet on the ramp. AR, dip in the autochthon. ML, Mountain Limestone (Namurian). (b) Rotation into the horizontal of the axes of the cross folds A and B and consequent rotations of the remaining points (1, plotting of the line LO, see text). (c) Unfolding of the La Foz cross syncline by bringing F'_N and F'_S to the horizontal taking A′ and B′ as rotation axes. (d) The same rotations as before to measure the strike and dip of the ramp cropping out in the southern limb of the La Foz cross syncline. (e) Field data (average values) in the Felechosa syncline. F_N and F_S, dips of the fold limbs measured in the autochthon. R_S and R_N, dips measured in the thrust sheet. E, axis of the cross fold. EL, Escalada limestone (Moscovian) (f). Rotation into the horizontal of the E axis and rotation of the southern limb F_S to the horizontal.

O and L in Fig. 4a) through a distance of 2 km. The trace of this line (l, Fig. 4b) in the restored ramp (L'', Fig. 4c) gives an apparent dip for the ramp of 11°17', which means that the ramp crosses 2000 × sin11°17' = 391 m of 'Mountain' Limestone, which is a value close to the known thickness of this formation in the area.

Another ramp can be seen below the Rioseco sheet in the southern limb of the syncline, where the overthrust surface cuts across the beds above the Escalada Limestone (Figs. 3 and 4a). Unfolding the syncline in the same way as before (Fig. 4d) the following results were obtained:

N29°E, for the ramp direction, deduced from the intersection between the Rioseco overthrust surface (parallel to bedding) and the bedding in its autochthon.

8°, for the ramp dip.

The direction obtained is not far from that described above, indicating a consistency in the results.

In the Felechosa syncline (Fig. 4e), the ramp can also be seen below the Rioseco thrust sheet. Figure 4(f) shows the field data and the analysis used to restore the thrust sheet to its former position. The results obtained are:

W18°N, for the ramp direction and

13°, for the ramp dip.

The ramp direction is very different from those obtained before, but this direction can be explained as being the result of the arcuation of the structures. The ramp strike curves through 86° from the northern limb of the La Foz syncline to the southern limb of that one of Felechosa.

The body of the nappes

The Cantabrian nappes have moved without being internally folded. The internal structure is very simple and, disregarding the effects of later folding, the nappes can be considered as large flat plates, essentially parallel to bedding. The only fold structures that occur are flat-topped anticlines due to thickening of the sequence as a consequence of tectonic overlapping, as in the classical examples in the Appalachians (Rich 1934, Butts 1927, Wilson & Stearns 1958, Rodgers 1963). The flat-topped anticlines are generally no longer recognizable because they have been too strongly modified by later folding; nevertheless, the eroded antiforms giving tectonic windows probably coincide with some of these older structures or with duplexes, folded forming antiformal stacks.

Foot-wall ramps

Any ramp, cutting up-sequence, produces the truncation of the beds below. In the Cantabrian zone, the best examples to be observed are those below the above measured ramps of the Laviana, Rioseco and Espinaredo overthrusts (Fig. 3). In the first, the beds below the ramp are bent in a syncline which is cut by the ramp. This syncline is not continuous all along the foot-wall ramp. In the other two cases, the beds are not folded.

Hanging-wall ramps

Because of their rather frontal position within the nappe, in the Cantabrian zone the hanging-wall ramps have been eroded. Only in two localities have they been preserved. These localities are in the Somiedo–Correcilla unit, east from Getino, and in the frontal part of the Esla nappe (Fig. 5).

In the Somiedo–Correcilla unit, the hanging-wall ramp can be seen south from Getino, where the thrust surface shears up-sequence through the bedding of the nappe to flatten at the base of the Santa Lucía Limestone (Emsian–Couvinian) and to rest on the Carboniferous. According to Rich's model, and disregarding later folding effects, a gentle inflexion of the beds corresponding to the frontal limb of a more or less wide, flat-topped anticline and bounded by an 'anticline' and a 'syncline' hinge might be expected. What is in fact found is an anticline and a syncline with a small interlimb angle (20°) (Fig. 5).

In the Esla nappe the overthrust surface cuts across the nappe bedding until reaching the base of the Santa Lucía Limestone, where it is again parallel to bedding. At the level of the Arenigian Barrios Quartzite the beds bend through an angle of 90° and are intersected at a high angle by the overthrust surface (hanging-wall ramp). Above the Barrios Quartzite, the Silurian and Devonian beds are affected by several folds with interlimb angles of about 60°. These folds have been later crossfolded. The restoration to their original position, made by Arboleya (1981), showed a N128°E original axial trend.

Thus, the beds above both hanging-wall ramps have similar characteristics and show much tighter folds than could be expected from Rich's idealized model of a thrust sheet being translated over a surface composed of ramps and flats.

A GEOMETRICAL TWO-DIMENSIONAL MODEL FOR THE CANTABRIAN NAPPES

Although conforming essentially to Rich's model for the Appalachians, in the Cantabrian nappes there are some special features which need to be explained; for example, the tightness of the folds above the hanging-wall ramps.

Theoretical hanging-wall geometry in nappes initiated as thrusts cutting across flat-lying beds

First consider a thrust plate initiated without being associated with any previously developed fold, subjected only to uniform horizontal translation with a motion normal to the ramp strike and with plane-strain conditions prevailing during nappe emplacement. If the rocks show no significant strain and the original thickness of the beds has been preserved (as in the case of the

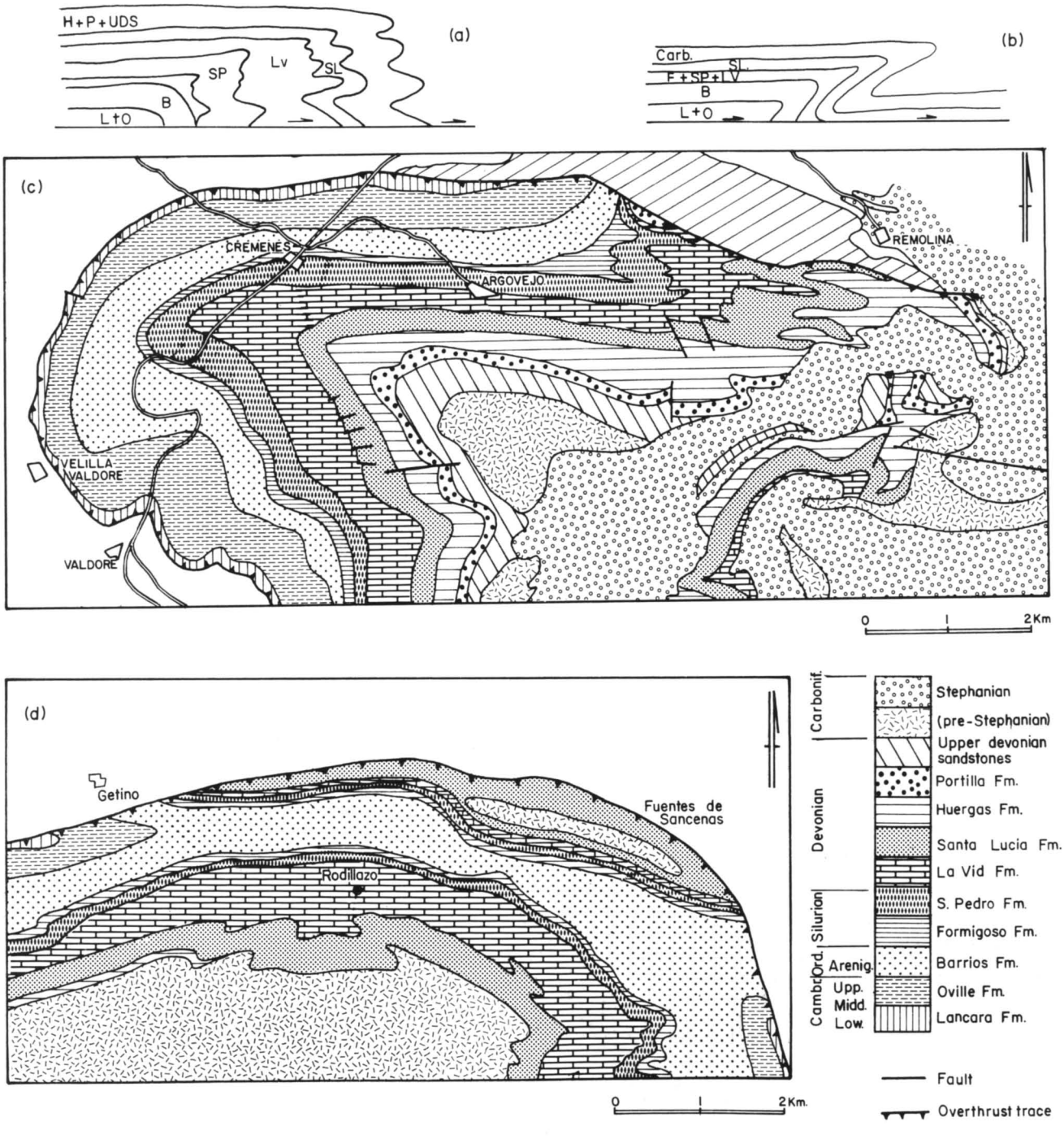

Fig. 5. Folds above the hanging wall ramp in the Esla nappe (a and c) and in the Correcilla Unit (b and d). The autochthone has been left in white. a and b: cross sections restoring the thrust surfaces to the horizontal. Map areas labelled B and C in Fig. 1.

Cantabrian nappes), the angle between bedding and the hanging-wall ramp will be a function of the ramp dip. Figures 6(a) and (b) show two profile models of the type of geometry expected in this situation. In each model, the area above the hanging-wall ramp (DEF) must be equal to the area of the triangle ABC, below the foot-wall ramp. Thus, from Fig. 6(a) (giving β in radians):

$$\frac{\beta t^2}{2} - \frac{t^2}{2 \tan \beta} = \frac{t^2}{2 \tan \alpha}$$

and simplifying:

$$\cot \alpha = \cot \beta + \beta. \quad (1)$$

For the particular case of Fig. 6(b), $\beta = \pi/2$ and consequently $\tan \alpha = 2/\pi$, which means that the model of Fig. 6(b) will be possible only for values of $\alpha = 32.5°$. If α takes on higher values there will be lack of material above the hanging-wall ramp, and some kind of special geometric accommodation is required. However, foot-wall ramp angles higher than 32° are not to be expected. A similar treatment by Suppe & Namson (1979) but considering a chevron geometry gives a similar result of $\alpha = 30°$.

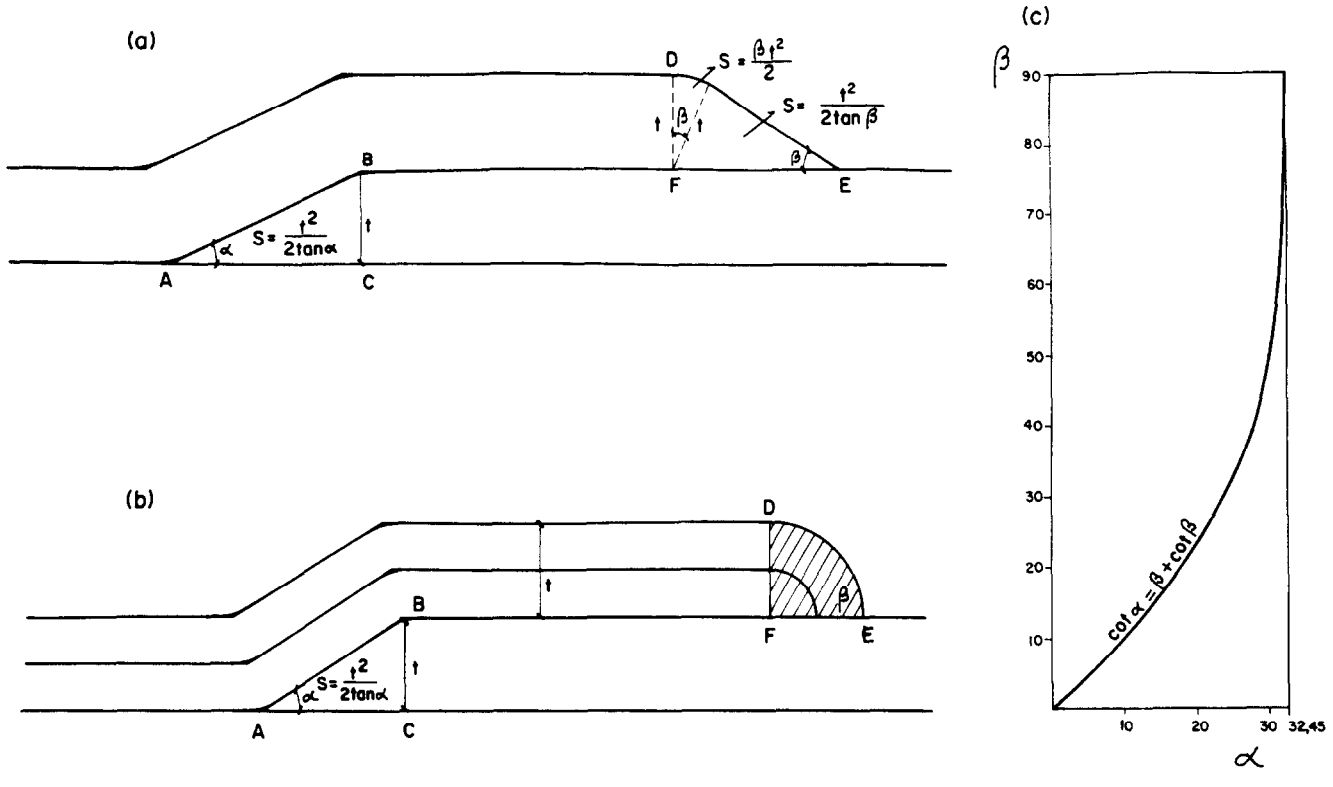

Fig. 6. Two-dimensional theoretical models of a décollement nappe, considering that the nappe has been subjected solely to uniform translation. S, area. See text for details.

Figure 6(c) records graphically the solutions of the above equation for values of β from 0° to 90°; it is seen that for $\alpha < 15$–$20°$, $\beta \cong \alpha$, but for higher foot-wall ramp angles the β values increase greatly with small α increments, until reaching $\beta = 90°$ for $\alpha = 32.5°$.

Thrusted folds

If a model of thrust plates initiated from folds is considered, the folds will be a train of tight, quite narrow anticlines separated by broad, flat-bottomed synclinal areas. The existence of a sequence of thrusts implies a periodicity in the anticlines, and the ramp and flat geometry implies the existence of broad flat areas between the anticlines. Downwards, these folds have to die away to a décollement surface placed immediately below the layers mechanically controlling the shape and wavelength of the folds.

In Figs. 7(a) & (b), two very simple models of concentric folds with a single centre of curvature have been represented. Assuming that their shape and wavelength have been controlled by bed 0, and that the thickness of the beds above remains constant, the fold wavelength increases upwards while the dip on each limb decreases. Nevertheless, for the model to be geologically realistic, the shortening produced must be the same in the different beds. The length L_0 and L_1 of beds 0 and 1, between AA′ and BB′, in Fig. 7(b), making $t_0 = 1$, will be:

$$L_0 = 2a + 2\varphi$$

$$L_1 = 2\alpha(1 + t_1)$$

and as

$$a = (t_1 + 1)\sin\alpha - \sin\varphi$$

it results that

$$L_0 - L_1 = 2(\varphi - \sin\varphi) + 2(1 + t_1)(\sin\alpha - \alpha) \quad (2)$$

α and φ being related according to the equation

$$\cos\varphi = (t_1 + 1)\cos\alpha - t_1$$

as deduced from triangles A′CD, FOE and DOE. Equation (2) always takes positive values, indicating that in the model bed 1 is consistently shorter than bed 0.

Taking a tighter fold (Fig. 7a) the conclusions would be the same. In this model, $\varphi = \pi/2$ and $t_1 = 1/(\sec\alpha - 1)$. Substituting in equation (2) and simplifying

$$L_0 - L_1 = \pi + 2\left(\frac{\tan\alpha - \alpha}{\sec\alpha - 1} - \alpha - 1\right). \quad (3)$$

If bed 2 is considered in the same way, taking α' instead of α, using $T = t_1 + t_2$, and considering the length between CC′ and DD′, a similar equation is obtained. This indicates that the length difference depends only upon the angle α which is a function of the total thickness T, and is independent of how many beds are considered. The model is not stable geometrically; the beds above bed 0 must suffer additional shortening, either by thrusting and telescoping or by additional folding.

Another fold model is represented in Fig. 7(c). Using the same geometrical model proposed by Ramsay (1974), but considering an isolated chevron fold, it is seen that there are some differences (for example the axial planes are diverging upwards) which make the

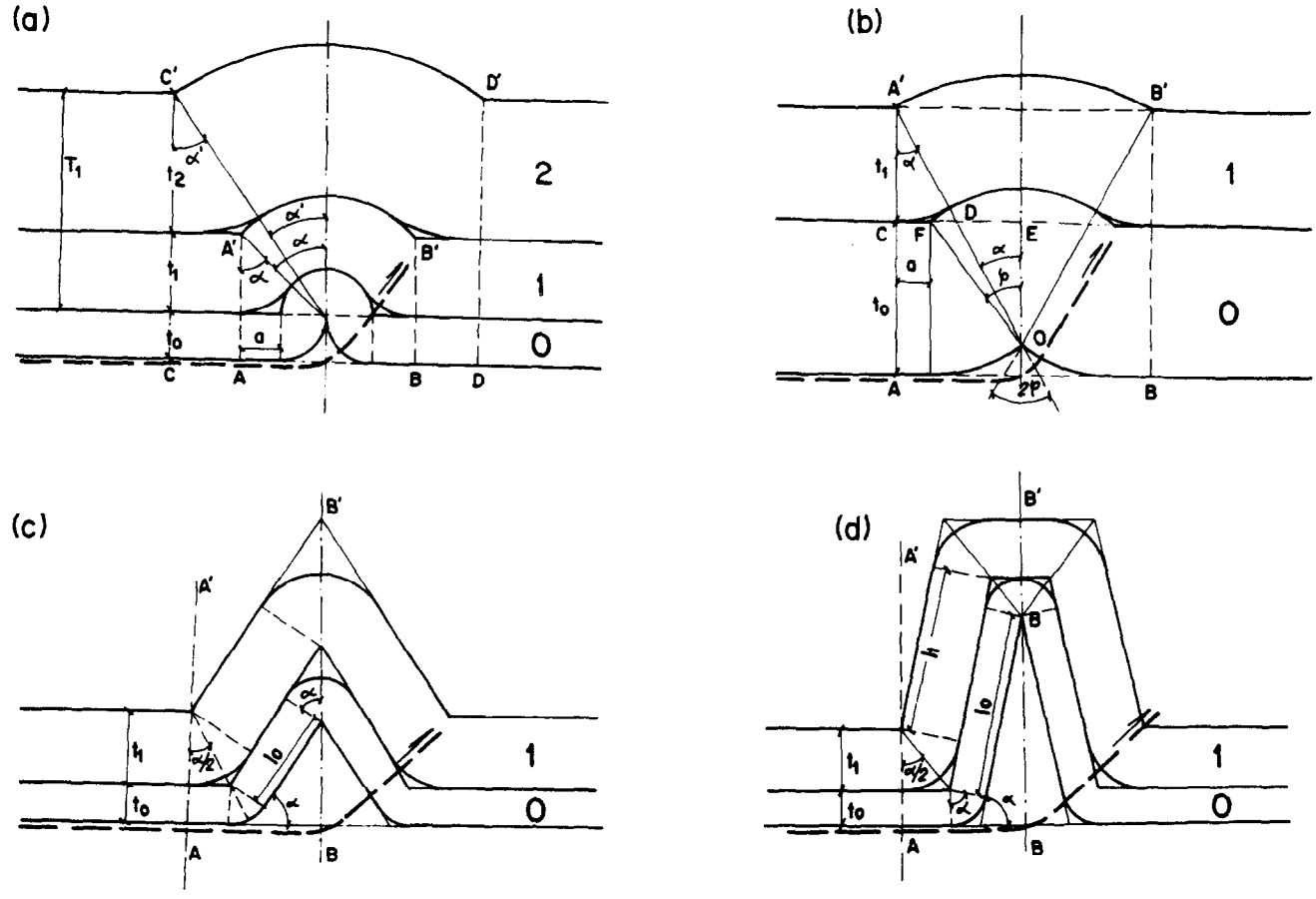

Fig. 7. Geometrical models of isolated folds. See explanation in the text.

model unstable. In this model the beds have increasing length upwards.

A stable model can be drawn with a box fold geometry (Fig. 7d). In this model the length difference between L_0 and L_1, measured from AA′ to BB′, is

$$L_0 - L_1 = 2 \tan \frac{\alpha}{2} (t_1 - t_0) - \alpha(t_1 - t_0). \quad (4)$$

This function is zero for $t_0 = t_1$, indicating that the model is stable with beds of constant thickness. This is probably the reason that box fold geometry is frequently found in folded sequences underlain by a décollement surface (Jura mountains, for example), and in isolated folds produced experimentally. If $t_1 > t_0$, $L_1 > L_0$ and the thickest bed has to be accommodated, for example by the thrusting of the flat top of the fold over one of its limbs.

The above models are very simple; nevertheless they seem to indicate that the structure of narrow anticlines separated by wide flat-bottomed syncline areas is not stable through the stratigraphical sequence. The wavelength of the anticlines increases upwards, and in addition the beds above have to suffer extra shortening, except in the case of box folds. As a result, there should exist a more or less continuous train of folds at a certain distance above the décollement surface.

Comparison with the Cantabrian examples

As a general rule, the origin of the ramps as thrusts cutting across undeformed flat-lying beds, rather than as thrusts cutting across limbs of isolated folds, is postulated for the Cantabrian nappes. The reasons are as follows:

(1) If a thrust sheet originated by cutting across a limb of a fold, and if it had been subjected solely to translation, synforms would be expected below the foot-wall ramp. Similarly, more or less bulbous-shaped antiforms would be expected above the hanging-wall ramp. Such structures are not observed in the Cantabrian nappes.

(2) Except in a part of the Rioseco thrust sheet, the beds below the foot-wall ramp are planar, cut by the overlying thrust, and no synclinal forms are observed.

(3) Even where the nappes rest on high levels of the Palaeozoic sequence, the overthrust surface and the bedding below are essentially parallel.

These conclusions are in accordance with the types of small-scale structures observed: wedging (Cloos 1961) and small telescoping of competent beds, formed during an early stage of deformation are common throughout the Cantabrian zone (Fig. 8f).

Nevertheless, the tightness of the folds above the hanging-wall ramps cannot be explained by simple translation of the thrust sheet. The shape modification could be due to drag taking place mainly at the ramps, as proposed by Berger & Johnson (1980). Nevertheless, the Cantabrian folds have no bulbous shape (Fig. 4) and furthermore in the Esla nappe there are several folds, indicating that the beds have been contracted. These structures are best accounted for by shape change of the

beds above the hanging-wall ramp by simple shear during nappe emplacement. This mechanism was also suggested by Suppe & Namson (1979) to explain some peculiarities of the frontal folds of the western Taiwan fold-and-thrust belt. This simple shear was parallel to bedding through most of the nappe body, as indicated by Elliott (1976).

The beds above the hanging-wall are oblique to the overthrust surface and to the simple shear direction; consequently they rotate into the contraction field of the finite strain ellipsoid and become folded. A slaty cleavage tilted by later folding is observed in some areas, and can be interpreted as related to shear parallel to bedding. The shear may be calculated by using the folds above the hanging-wall ramps and the slaty cleavage in the body of the nappes.

In the Esla nappe, several folds are present, particularly in the Devonian formations. As the axes of the folds are essentially parallel, the contraction can be evaluated, and the value obtained is $e = (l_1/l_0) - 1 = -0.4$. If the folds were generated by simple shear parallel to bedding l_0 is measured along the line DE in Fig. 6, and as the thickness (t) is known, the angle β can be calculated, giving a value of $\beta = 33.3°$. Furthermore, from this value, using eqn (1), the ramp angle can be also calculated; the value obtained is $\alpha = 25.4°$, which is in accordance with the figures found from field data. The angle β is the theoretical angle between bedding and the overthrust surface at the hanging-wall ramp, disregarding the effects of simple shear. On the other hand, the envelope of the fold train forms at present an angle of 70° with the overthrust surface. Thus, by using the equation $\gamma = \cot \alpha' - \cot \alpha$ (α and α' being the angles of a line with the shear direction before and after shearing; 33.3° and 70° in the present case) the values $\gamma = 1.16$ and $\psi = 49.3°$ are obtained for the shear strain and the angular shear, respectively.

By using the slaty cleavage contemporary with the nappe emplacement, similar figures are found. The best example is provided by the tilted cleavage along the eastern limb of the Narcea antiform, visible in some localities in its southernmost part. In the locality of Irede, bedding and cleavage form an angle of 25°, and the intersection line trends 295°. Assuming that the cleavage was generated by simple shear parallel to the bedding, values of $\gamma = 1.14$ and $\psi = 48.7°$ are obtained.

THE LATERAL DYING OUT OF THE NAPPES: THEIR THREE-DIMENSIONAL GEOMETRY

At the end of an overthrust the thrust fault has to pass into some other kind of structure which can absorb the shortening produced; such a structure may be a strike-slip fault or a fold system, as shown by field data and laboratory experiments (Gardner & Spang 1973).

In several localities, the Cantabrian thrust sheets die out laterally into folds. This relationship is best observed in the fold and nappe province, where there is a change from southeast to northwest from overthrust to fold structure. Very good examples are provided by the northern extremities of such thrust sheets as those of Belmonte, Tameza and La Sobia (Fig. 9).

From these and other examples, the following characteristics are deduced.

(1) In simple cases, an individual thrust sheet dies out against an anticline–syncline couple.

(2) The thrust can end in the core of a fold. This fold can be either an antiform or synform.

(3) The folds into which a thrust dies out always have axial directions oblique to the thrust direction.

(4) When the thrust ends in an anticline core (the common case in the Cantabrians), the angle between the fold axis and the overthrust trace measured on the hanging-wall side of the overthrust is larger than 180°.

(5) When the thrust ends in a syncline core (uncommon in the Cantabrians) the angle between fold axes and overthrust surface measured on the hanging-wall side is smaller than 180°.

(6) The axes of the syncline and anticline absorbing the shortening at the end of an overthrust can be parallel or converging (diverging against the thrust and converging in the opposite direction).

(7) The folds at the end of an overthrust are rather tight (30–65° interlimb angle) and have narrow hinge zones and straight limbs.

Geometrical analysis

It will be assumed that the folds into which the overthrust dies out are completely angular, that the surface considered has not been strained, neither in the fold system nor in the thrust plate, that the back limb of the anticline is horizontal, and that the thrust plate has moved together with the back limb of the anticline. These conditions fit the field data quite well for, although the folds at the end of the overthrusts have been somewhat flattened and show a weak cleavage, the shape change is very small.

If the syncline and anticline axes at the end of a thrust sheet are parallel, the horizontal slip (AB) and the amplitude of overlapping (AD) measured normal to the overthrust strike will be respectively (see Fig. 10a)

$$AB = c(1 + \cos \beta) \quad (5)$$

$$AD = c(1 + \cos \beta) \cos \alpha, \quad (6)$$

c being the distance from the anticline to the syncline hinge, β the angle between limbs and α the angle between fold and thrust strike. From the above equations the following points are deduced. (1) The lengths AB and AD remain constant along the thrust strike. (2) The theoretical maximum value for AB is $2c$, when $\beta = 0$, and the fold is then isoclinal. (3) AD diminishes as α increases, so that AD = 0 when $\alpha = 90$ (fold ending against a strike-slip fault). (4) The maximum value of AD will be when $\alpha = 0$, but in this case SA = ∞; this means that it is not possible to pass from a fold to an overthrust if their trends are parallel, unless

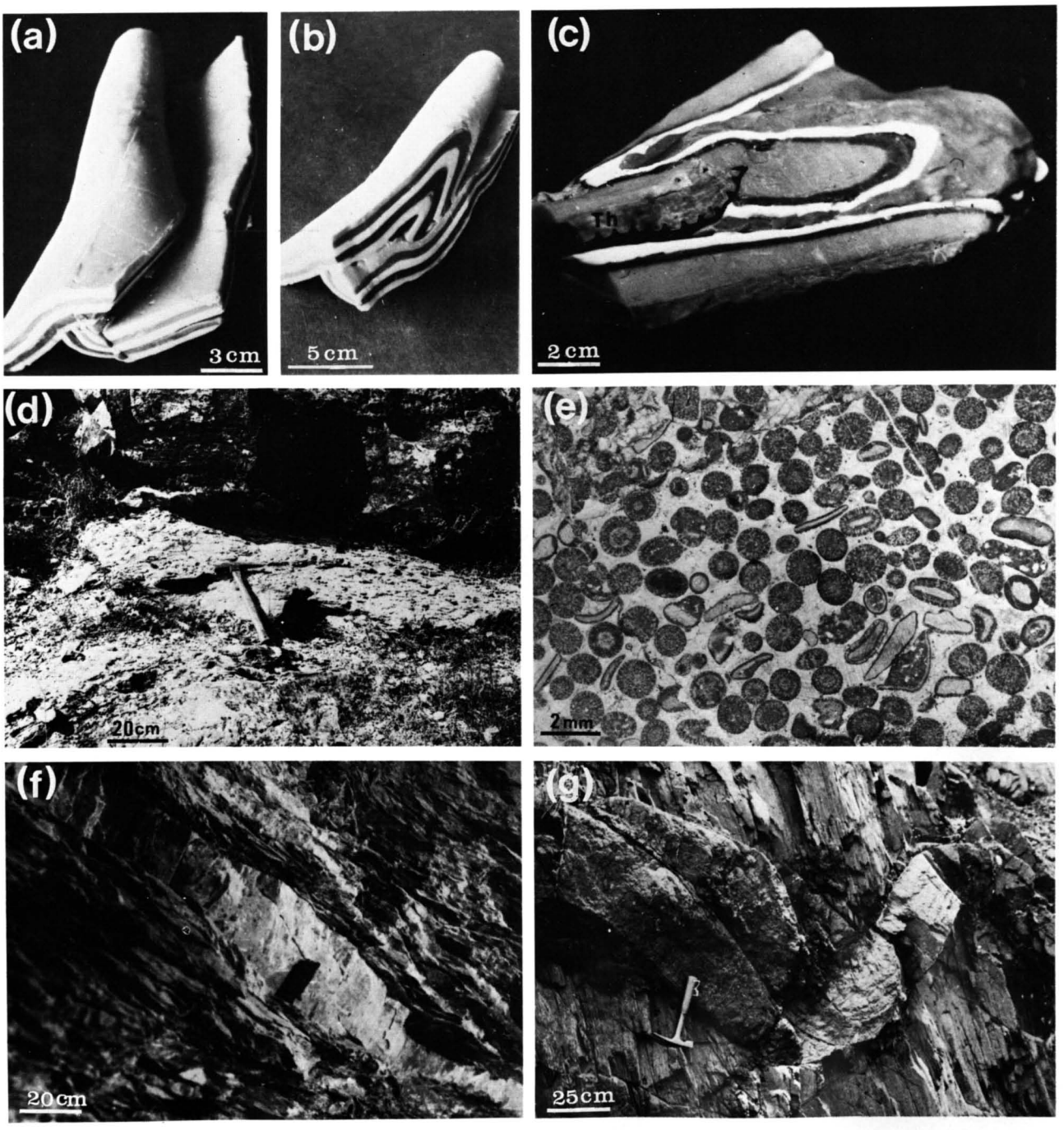

Fig. 8. (a) Plasticine model of a thrust ending in a syncline core. (b) The same model cut to show the cartographic pattern. (c) Plasticine model of a thrust ending in an anticline core. (d) Deformed zone at the base of the Esla nappe in the locality of Valdore. (e) Undeformed oolites in the Lancara formation 20 m above the overthrust surface. (f) Wedge in a sandstone bed in the Cape Peñas area. (g) Folded wedge with an axial plane slaty cleavage near the Cape Peñas.

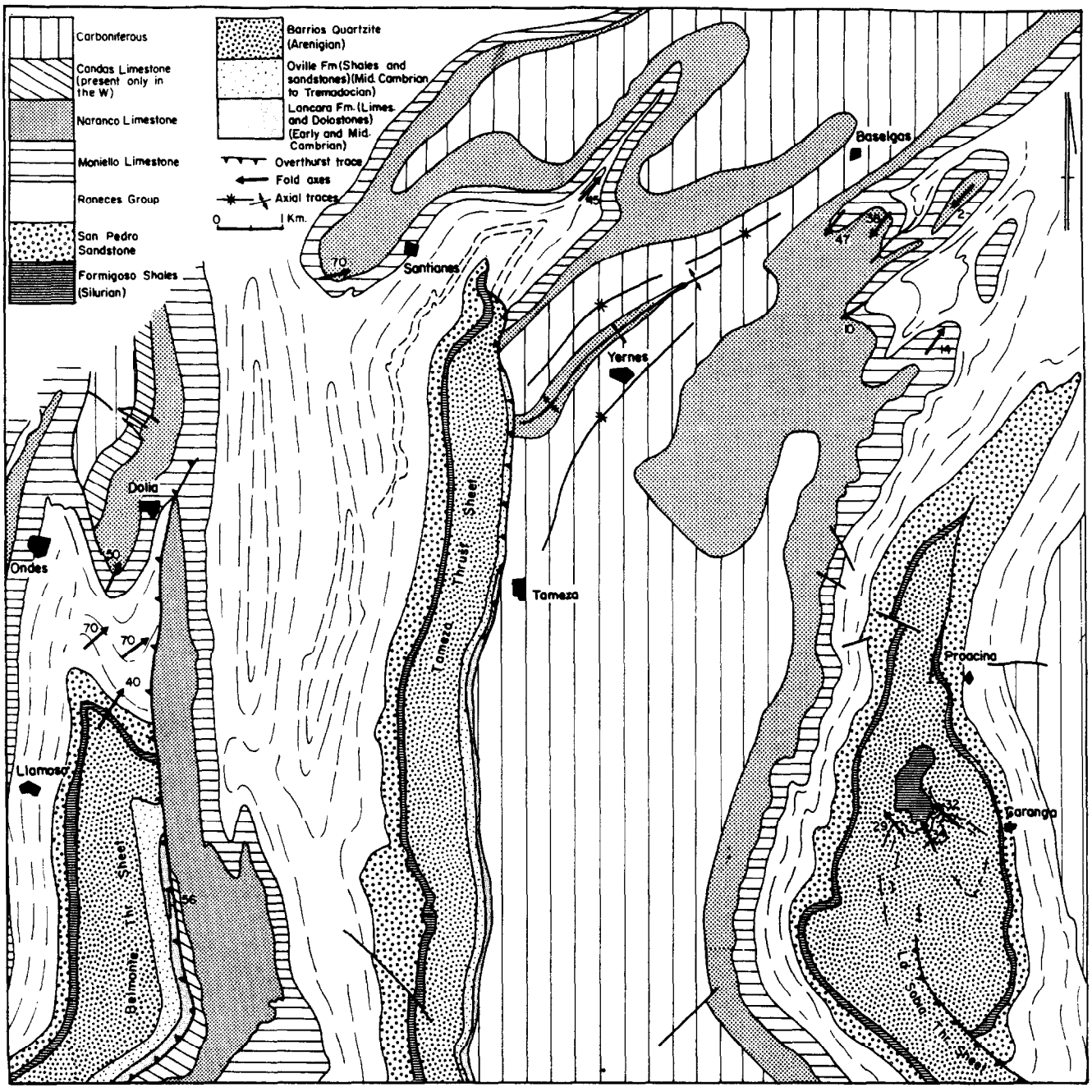

Fig. 9. Northern extreme of the Belmonte, Tameza and La Sobia Thrust sheets showing their lateral dying out into folds. Map area labelled D in Fig. 1.

the plate is strained or a strike-slip fault develops at the boundary between overthrust and fold system. (5) The amplitude of the overlap depends largely on the length of the reverse limb of the anticline at its end, and consequently it cannot be very large except in the case of a large recumbent anticline; such situations are not found in the Cantabrians. (6) The horizontal net slip is oblique to the overthrust strike.

If the anticline and the syncline axes converge outwards from the overthrust surface, the equations giving the horizontal net slip (AB) and the amplitude of overlapping (BD) at the point where the thrust joints the anticline hinge are (Fig. 10b)

$$AB = c \frac{\sin \alpha}{\sin \alpha'} (1 + \cos \beta) \qquad (7)$$

$$BD = c \frac{\sin 2\alpha}{2 \sin \alpha'} (1 + \cos \beta). \qquad (8)$$

Although the above functions have four variables (α, α', c and β—see Fig. 10(b) for their significance), α and α' are the most geometrically significant, and c and β will therefore be considered as constants. This matches quite well the folds at the end of the Cantabrian overthrusts which have rather similar size and interlimb angle. Thus, horizontal net slip and amplitude of overlap will be analysed as functions of the angles (α and α') between the thrust directions and the syncline and anticline axes or, alternatively, as functions of one of these angles and the angle between both fold axes ($\theta = \alpha - \alpha'$).

Equations (7) and (8) have geological meaning for $90 \geqslant \alpha \geqslant \theta$; thus, they will be considered only within

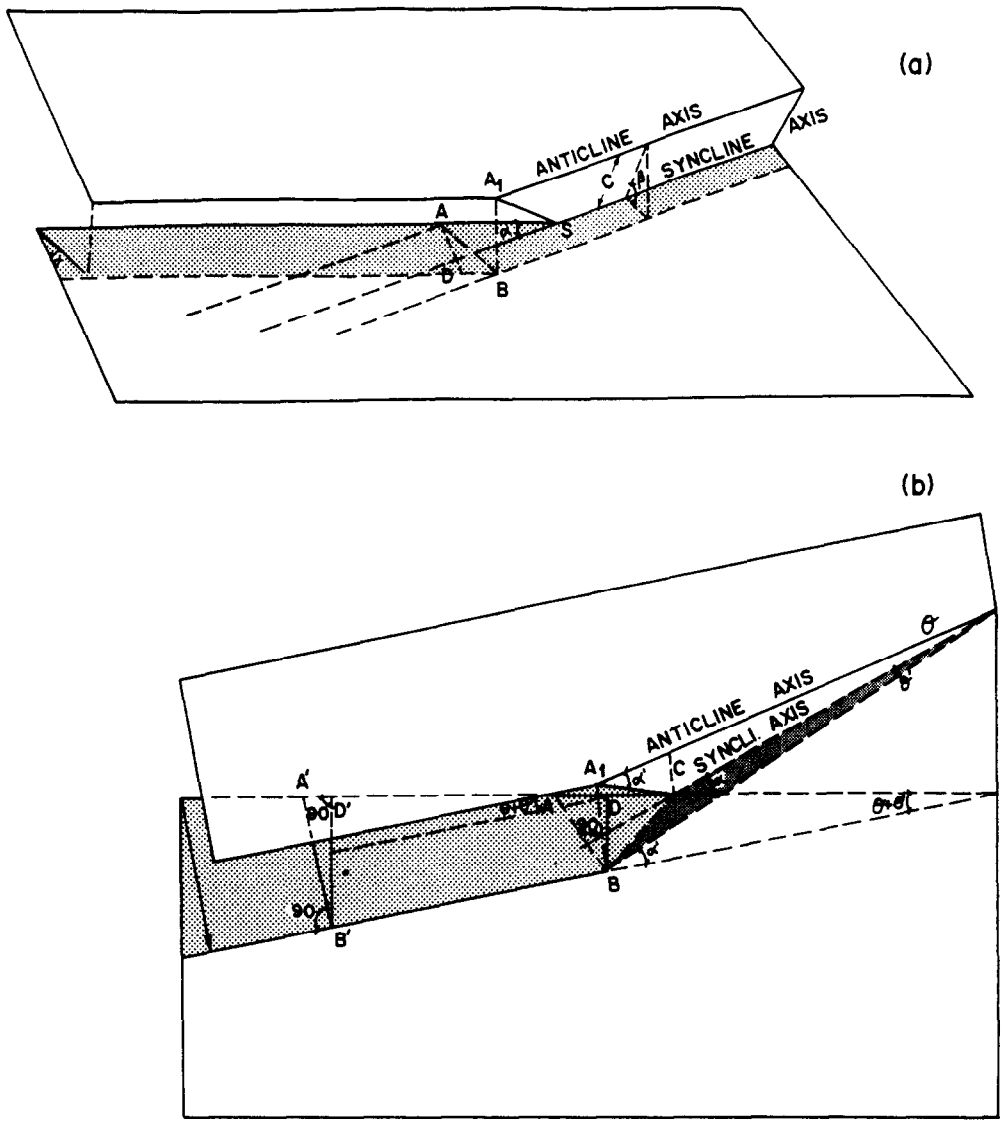

Fig. 10. (a) Thrust ending against an anticline–syncline couple with parallel axes. (b) Thrust ending against an anticline–syncline couple with diverging axes.

this interval. From (7), making $c = 1$, β = constant (and $<90°$), AB = y, and differentiating with respect to α and θ:

$$\frac{\partial y}{\partial \alpha} = \frac{\sin \theta(1 + \cos \beta)}{(\sin \alpha \cos \theta - \sin \theta \cos\alpha)^2} \tag{9}$$

$$\frac{\partial y}{\partial \theta} = \frac{(1 + \cos \beta) \sin \alpha(\sin \alpha \sin \theta + \cos \alpha \cos \theta)}{(\sin \alpha \cos \theta - \sin \theta \cos \alpha)^2}. \tag{10}$$

As $\partial y/\partial \alpha < 0$ and $\partial y/\partial \theta > 0$, AB increases with decreasing α and increasing θ values. It can be also deduced that for $\alpha = \theta$ the function is discontinuous. The geological meaning is that the horizontal net slip at point B (or A1) progressively increases with higher values of θ and lower values of α. Where $\alpha = \theta$ the intersecting line of the thrust surface and the bedding in the hanging-wall is parallel to the anticline axis. In consequence the structure becomes an anticline with a thrust reversed limb, and does not correspond to the model. For higher values of θ the equation has no geological meaning. If $\alpha = 90$, the horizontal net slip at point B (or A1) coincides with the strike of the ramp. The amplitude of overlap (BD) also increases with the increase of θ or decrease of α. Although equations (7) and (8) have geological meaning in the interval $90 \geqslant \alpha \geqslant \theta$, the field evidence in the Cantabrians shows low θ ($30 \geqslant \theta \geqslant 0$) and moderate α ($60 \geqslant \alpha \geqslant 40$) values.

Equations (7) and (8) give the horizontal net slip and the overlapping amplitude in the merging point of thrust trace and anticline axis, but away from this point, along the overthrust, the values increase progressively. Thus, for a given structure the equation to calculate the amplitude of overlapping (B'D') as a function of the distance to point B is:

$$B'D' = BD + BB' \sin (\theta + \theta') \tag{11}$$

or, making B'D' = u, and BB' = x:

$$u = c \frac{\sin 2\alpha}{2 \sin \alpha'} (1 + \cos \beta) + x \sin (\theta - \theta'). \tag{12}$$

For a given structure α, α', β, θ and θ' are constants and equations (11) and (12) take on the forms of straight lines, BD being the ordinate at the origin and $\sin(\theta + \theta')$ the slope. This means that there is a linear relationship between the distance to the overthrust–anticline merging point and the overlapping amplitude, and that the slope of the line depends on the angle (θ) between anticline and syncline hinges and the interlimb angle [$\theta' = f(\beta, \theta)$].

The horizontal net slip will also increase with the distance to point B, and the slip direction will be progressively less oblique to the ramp direction. The actual displacement path of a point in the nappe will be rather complicated. If the vertical component of the displacement path due to the ramp is neglected, the nappe movement will be a rotation around a centre placed at the converging point of the anticline and the syncline hinges, situated at the end of the nappe. Where the distances to point B are large this simplification seems geometrically reasonable. In the experiments carried out by Gardner & Spang (1973, plates 1 and 3), a rotation of the thrust plate is also observed.

It follows from the above equations that an overthrust with a large overlap can lose importance in a rather short distance and can die out in a system of folds of small or moderate size.

Finally, because an overthrust has two ends it is necessary that some kind of deformation inside the body of the thrust sheet exist. In that case the overlap amplitude will be given by a non-linear function $u = f(x)$, in which $du/dx < \sin(\theta + \theta')$. However, for low x values du/dx will approach $\sin(\theta + \theta')$ and the relationship will be nearly linear. As x increases, the difference, $\sin(\theta + \theta') - du/dx$, also increases and du/dx approaches zero; the maximum overlap ($du/dx = 0$; $d^2u/dx^2 > 0$) will be reached at approximately half the distance between the ends of the overthrust (Elliott 1976; see also experiments by Gardner & Spang 1973).

Even though the Cantabrian overthrust sheets show large overlaps, no important internal deformation contemporary with their emplacement has been recognized. The problem will be fully discussed later, after defining the true trace of the Cantabrian thrusts.

The Cantabrian examples

The examples in the Cantabrians which most nearly conform to the above geometric models are shown in Fig. 9. Among them, the best are probably the Belmonte and Tameza thrust-sheets, corresponding respectively to a thrust ending in a syncline and an anticline. In the Belmonte overthrust, folds occur in the hanging wall. The overthrust cuts across an anticline and comes to an end in a syncline. In the foot-wall the bedding is more or less parallel to the overthrust. The formation where the thrust ends (Moniello Limestone) shows a Y pattern on the map (near Dolia, Fig. 9) a feature characteristic of thrusts ending in a syncline (compare with the plasticine model of Fig. 8).

According to the geometrical models, such an end implies that the angle between fold axes and the thrust direction is less than 180° (measured in the hanging-wall side of the thrust). Restoring the overthrust to the horizontal, the folds are brought also nearly to the horizontal, as expected from the model, and form an angle $\theta = 10°$. The values of the angles α and α' are somewhat uncertain but it seems probable that α varies between 54 and 60° and α' between 50 and 44°. The present angle β is 30.4° although it may have been modified during the phase of overthrust folding and $c = 1052$ m.

In contrast to the Belmonte thrust, the Tameza thrust dies out into an anticline. The thrust and fold directions form an angle smaller than 180° (about 130°, measured in the foot-wall of the thrust); hence, the folds cut by the thrust are found in the foot-wall side, whilst the hanging-wall is not folded and bedding is parallel to the thrust. The cartographic pattern corresponds perfectly to the plasticine model (Fig. 8).

Further east, the La Sobia thrust also ends in an anticline. In this example although no firm value for θ can be obtained it seems to be very low. If it can be assumed that the anticline and syncline axes are subparallel, the angle between thrust direction and fold axes will be $\alpha = \alpha' = 30°$.

It is emphasized that the equations above were developed for a model consisting of a thrust ending against a syncline axis. If the thrust ends in an anticline the equations remain valid provided that the meaning of the symbols remains unchanged. For example, α is now the angle formed by the thrust direction and the anticline axis and α' the angle with the syncline axis. The angle α is always measured between the thrust direction and the axis of the fold into which the thrust dies out. From the calculated values of α, α', θ, β and c, use of equations (7) and (8) enables AB and BD to be calculated for several structures. The values obtained have been plotted in Fig. 11(b).

Fold systems at the overthrust termination and lateral extension of the nappe

In the above examples only the anticline–syncline couple at the very end of the thrust has been considered. Nevertheless, in some cases there are more folds than a single syncline–anticline couple. An example is the northern extreme of the Tameza thrust. This ends in an anticline, but southeast of the anticline other folds exist in the foot-wall of the thrust. All these folds are restricted to the foot-wall side of the thrust and are cut by it. The hanging-wall, in contrast, is not folded and shows bedding parallel to the thrust. This indicates that the folds and thrust were contemporaneous.

The existence of a fold train at the end of a thrust can be interpreted as a consequence of its growth. A thrust starts in a given point and propagates from this point in all directions. The thrust spreads as the displacement at the starting point increases, but at a certain distance the thrust stops spreading and the shortening is absorbed by

the generation of a fold couple. With increasing thrust displacement the folds evolve, growing in amplitude and tightening. At some period the thrust cuts through the fold pair at its end and extends beyond it. Then the fold couple stops evolving and a new fold couple starts to develop at the new termination of the thrust. In this way a fold train, with progressively younger folds towards the thrust end, is formed.

The best example of the structure described is provided by the Tameza thrust, but other examples exist, as in the La Sobia–Bodón unit, along its contact with the central coal basin. The following succession of structures representing the lateral change from thrust to fold tectonics can be observed, as seen from southeast to northeast in the nappe and fold province:

(1) thrusts parallel to the bedding of the hanging- and foot-wall rocks, indicating that the thrust propagated without any associated folding (e.g. Esla nappe and eastern part of Bodón and Correcilla thrust sheets);

(2) thrusts parallel to the hanging-wall rocks and cutting a fold train in the foot-wall (or vice versa), indicating that the fault has extended progressively across a fold train as it was being formed; this disposition gives way to an area with coexisting thrusts and folds (e.g. northern part of the Tameza thrust, and in general all the middle part of the fold and nappe province where an interfingering of thrusts and folds exists);

(3) anticline–syncline pairs formed at the end of the thrusts, and

(4) folds rarely associated with a thrust, indicating that thrusting has not reached that area and that shortening was accomplished by folding (e.g. the northern part of the fold and nappe province).

STRAIN DISTRIBUTION IN THE CANTABRIAN NAPPES AND ASSOCIATED FOLDS

The strain within the body of the nappe

The body of the Cantabrian nappes is practically unstrained. Even the Láncara Formation at the sole of the nappes shows sedimentary structures perfectly preserved and undeformed (Zamarreño 1972, 1975). The existence of strained sedimentary structures in this formation has been recorded only in some localities very close to the Narcea antiform (e.g. deformed 'bird's eyes' in Villabandin, Zamarreño 1972). The existence in the shale horizons of a cleavage related to the nappe emplacement, as in Irede, is also exceptional. Nevertheless, from the folds above the hanging-wall ramps the existence has been deduced of simple shear parallel to the thrust surface affecting the body of the nappes. Thus, the simple-shear strain is not homogeneously distributed through the body of the nappes, but is inhomogeneous, with slip concentrated along particular bedding planes. The rocks forming the nappes, particularly the competent ones, remain unstrained. The nappes in the Cantabrians therefore differ from some other décollement nappes, like that of Glarus in Switzerland, in which the rocks clearly show strain (Pfiffner 1981).

Folds laterally equivalent to the nappes

In contrast to the nappes, the rocks in the folds do show some strain. The folds generally have straight limbs and relatively narrow hinge zones. Those measured at the very end of the nappes have interlimb angles of 30–65°, and similar values have been found farther north (30–60° in the Cape Peñas area, Julivert 1976); the commonest angles are 30–40°. The folds are flattened buckles with a weak cleavage. Nevertheless, strains determined from deformed fossils and sedimentary structures are small, especially in the limbs. The beds in the hinges are somewhat thickened and the limbs are boudinaged. There is also a system of conjugate normal kink bands and small shear zones intersecting at nearly right angles and bisected by the axial planes of the folds. The boudins, normal kink bands and shear zones are clearly related and were generated during the last stages of closure of the folds (Julivert 1976). They indicate a contraction normal to the axial planes of the folds and an elongation normal to their axes. An elongation fabric is also fairly prominent in the Cape Peñas, close to the Narcea antiform (elongated pyrite bodies with pressure shadows). However, here, the larger strains appear to be related to the start of metamorphism.

Before buckling, the beginning of contraction was accomplished by wedging and telescoping of the competent beds (Marcos & Arboleya 1975, Julivert 1976). Folded wedges with an axial plane cleavage can be observed in certain localities (Fig. 10; Julivert 1976).

The sole of the nappes

At the base of some of the Cantabrian nappes there is a thin layer in which the rocks have been strongly deformed. This deformation is considered to be associated with the advance of the thrust sheets on the substratum. The best example is situated at the base of the Esla nappe (Arboleya 1981), but other examples can also be seen at the base of the Correcilla thrust sheet and in some localities of the Ponga nappe. This layer is observed where the Láncara overrides another carbonate formation.

The deformation zones extend for a short distance above and below the thrust plane. In the Esla nappe, above the thrust plane is a zone of brecciated Láncara Limestone of 1 m thickness. The fragments, up to 2 cm in size, show the textural characteristics of the lower part of the Láncara Limestone and the groundmass consists of round quartz grains in a clay matrix. Above the breccia layer the Láncara Formation shows microfracturing, but the general texture of the rock is undisturbed; this microfracturing vanishes upwards at 3–4 m from the thrust surface. Similar breccias have also been found at the base of some other thrust sheets, such as the Correcilla unit. In this unit very thin cataclastic zones have been found some distances above the basal breccia, and separated from it by undisturbed rock.

Deformation below the thrust surface is greater than above. Grain-size reduction by cataclasis is clearly observed in all sections. Immediately below the thrust plane of the Esla nappe the deformed zone is 1 m in width and the rock shows a marked grain-size reduction. It is a light brown rock and shows a macroscopically visible cleavage which cannot be detected under the microscope. It is considered to have been formed by cataclasis of the Viséan limestone. Microscopic study has revealed the presence of a narrow central zone in which sliding deformation has given rise to an ultracataclasite. Symmetrically disposed at both sides of the ultracataclasite horizon, the grain-size reduction is less marked and the rock grades into cataclasites and protocataclasites. The matrix of the rocks of the cataclasite series is formed by clay minerals and rounded quartz grains. The origin of the quartz grains is uncertain; they are present only in the matrix and not in the porphyroclasts. This, together with the presence of similar grains in the breccias above the thrust plane and also of some sand dykes, suggests that the quartz has been injected from the underlying Upper Devonian sandstone during deformation.

In other localities the deformed zone below the thrust has a different character. In the Vegacervera section (Correcilla thrust) a 10 cm wide level of crush breccia is situated 30 cm below the thrust contact and two smaller zones of fine crush breccias are also found some centimetres below. Another manifestation of cataclasis is microfracturing of the rock up to 2 m from the fault contact. Further away no important deformation is observed.

The presence of the different rock types mentioned above shows that the deformation in the vicinity of the thrust plane has taken place under brittle conditions. This brittleness in the limestones must be closely related to the high pore pressure that existed at the base of the thrust plates during their emplacement.

NAPPE EMPLACEMENT AND ARCUATE TRACE OF THE FOLD BELT

Ramp directions along the Asturian arc

The arc, as it is now seen on the map, does not represent the true tectonic curvature of the structures. The arc shape is of composite origin and results from the superimposition of several kinds of structures. In addition, as a consequence of the intricate folding of the thrust sheets, the overthrust traces are not coincident with the true ramp or leading edge directions. To trace the true arc described by the thrust sheets and related folds, the real tectonic trends must be established. These may be: (1) the axial trends of the folds contemporary with the nappes, (2) the ramp directions in the thrust sheets, (3) the fold trends above the hanging-wall ramps and below the foot-wall ramps, and (4) the intersection lineation between bedding and the cleavage formed during nappe emplacement. Although the above structures have not the same exact genetic significance they mostly seem to have been generated during the same overall deformation period and so they will be used together to define the arc.

The data, shown in Fig. 11, are not sufficient to attempt an analytical solution to evaluate the maximum curvature, but an approximate evaluation has been made by finding the tangential circle touching to the tectonic arc at its hinge zone (Fig. 12). From Fig. 12 it is clear that the maximum curvature increases from west to east, being 2.5 times greater in the eastern boundary of the central coal basin than in the fold and nappe province.

The unfolding of the radial set of folds

The arcuate trace of the Hercynian orogen in NW Spain has attracted attention for many years, and different ideas have been given for its origin. More recently, Ries & Shackleton (1976), Ries *et al.* (1980) and Perroud & Bonhommet (1981) have discussed whether the arc is primary or secondary.

The existence of the radial set of folds vanishing westwards indicates increasing curvature as orogeny progressed (Julivert 1971b). The arc described by the first phase structures (thrusts and contemporary folds) as seen now had its shape modified by superimposition of later structures, mainly by superimposition of a radial set of folds. These folds are generally open and the shortening across them is about 40% in a N–S direction normal to the axial trace of the arc across the Ponga nappe province and the southern fold and nappe province. The shortening appears to be much less towards the west, where the radial set of folds vanishes; however measurements are more difficult to make.

From this restoration it can be shown (Fig. 12) that the curvature in the eastern border of the central coal basin increased nearly 3 times during the production of the radial folds. In contrast, in the fold and nappe province the curvature increased only about twice. Thus, discounting the effects of the radial set of folds, the curved shape of the structures remains, although the arc is more open.

The evolution of the arc has been analysed recently on the basis of paleomagnetic data (Ries *et al.* 1980) from NRM directions measured at 32 sites along the fold and nappe province. From the Cape Peñas to the Luna area the NRM shows a rotation of 110°. According to Ries *et al.* (1980) all magnetizations measured are of Variscan age (post-Early Carboniferous). New data were later published by Perroud & Bonhommet (1981) who also found an angle between NRM in the Cape Peñas and in the Luna area, although the value found was somewhat smaller (80°). Both groups of authors concluded that the curved shape of the structure is at least partially secondary in origin. According to Ries *et al.* (1980), the structures were bent 110° after magnetization, leaving an earlier arcuation of about 55°. According to Perroud & Bonhommet (1981), 80° of the curvature of the arc is secondary and 70° primary or pre-Carboniferous.

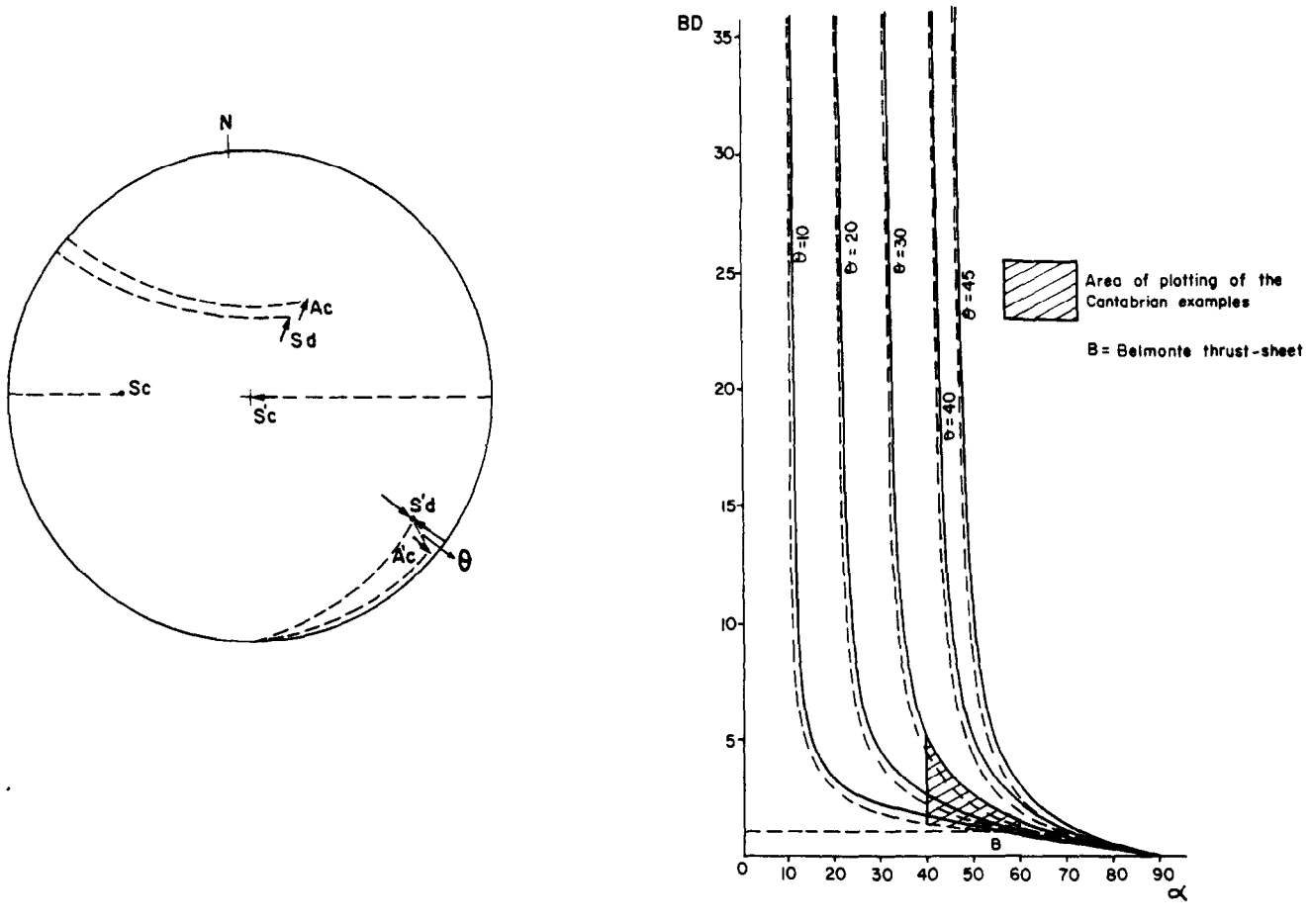

Fig. 11. Left, rotation into the horizontal of the Belmonte thrust sheet and resulting rotations in the folds at the end of the thrust. Sc, thrust surface. A_c and S_d, anticline and syncline at the termination of the thrust. θ, angle between anticline and syncline axes. Right, graphical solution of equation (8) for $\beta = 36°$ (full lines) and $\beta = 60°$ (dotted lines) and for successive values of $\theta(\theta = \alpha - \alpha')$.

Most of the NRM data quoted above are difficult to use for precise geometrical reconstructions. Besides problems such as sample treatment and age of magnetization, there is the difficulty of correctly restoring the bedding to its original position. Precise geometrical analysis has been done in some localities (Bonhommet *et al.* 1981), but in some cases the unfolding of the structures has not brought the magnetic vectors into alignment and, in most localities, the only correction has been a tilt correction rotating through a horizontal axis (Ries *et al.* 1980). Consequently the NRM data can only be used in a general way to understand the evolution of the arc.

We have shown that the shape of the arc before the radial folding can be evaluated (Fig. 12). If paleomagnetical vectors at the Cape Peñas and the Luna area are rotated accordingly, the remaining arcuation is 60 or 40°, depending on which datum (110 or 80°) is considered. This angle has to be explained by the effect of circumferential folding and nappe emplacement.

Variations of the horizontal net slip and the tectonic overlapping along the strike

According to the above analysis, the thrusts generated with a curved trace. The horizontal net slip and the overlapping amplitude given in eqns 11 and 12 are valid only for thrusts with slight curvature and short distances to the merging point with the thrust-termination fold.

In thrusts with curved traces, $y = f(x)$, which terminate in a fold couple with converging axes, the movement of the thrust plate is rotational according to an angle φ. Thus, the displacement of any point (x, y) to its new position (x_1, y_1) can be determined by rotating the coordinate axes through an angle φ and a new curve $y = g(x)$ can be obtained, representing the leading-edge trace (Fig. 13).

Each point has undergone a circular displacement, along an arc with its centre at the merging point of the converging folds (taken in Fig. 13 as the origin of coordinates). The horizontal net slip for successive points along the thrust trace is a vector with progressively greater length and forming a progressively greater angle (measured counterclockwise) with the X axis.

The area bounded by both curves has a crescent shape and represents the area where there is tectonic overlapping. Its shape indicates that, although the displacement grows progressively from the fold system at the end of the thrust, the overlap reaches a maximum at a certain point and then decreases to zero where the thrust trace coincides with the displacement path. The geological consequences are as follows: (1) the overthrust ends at

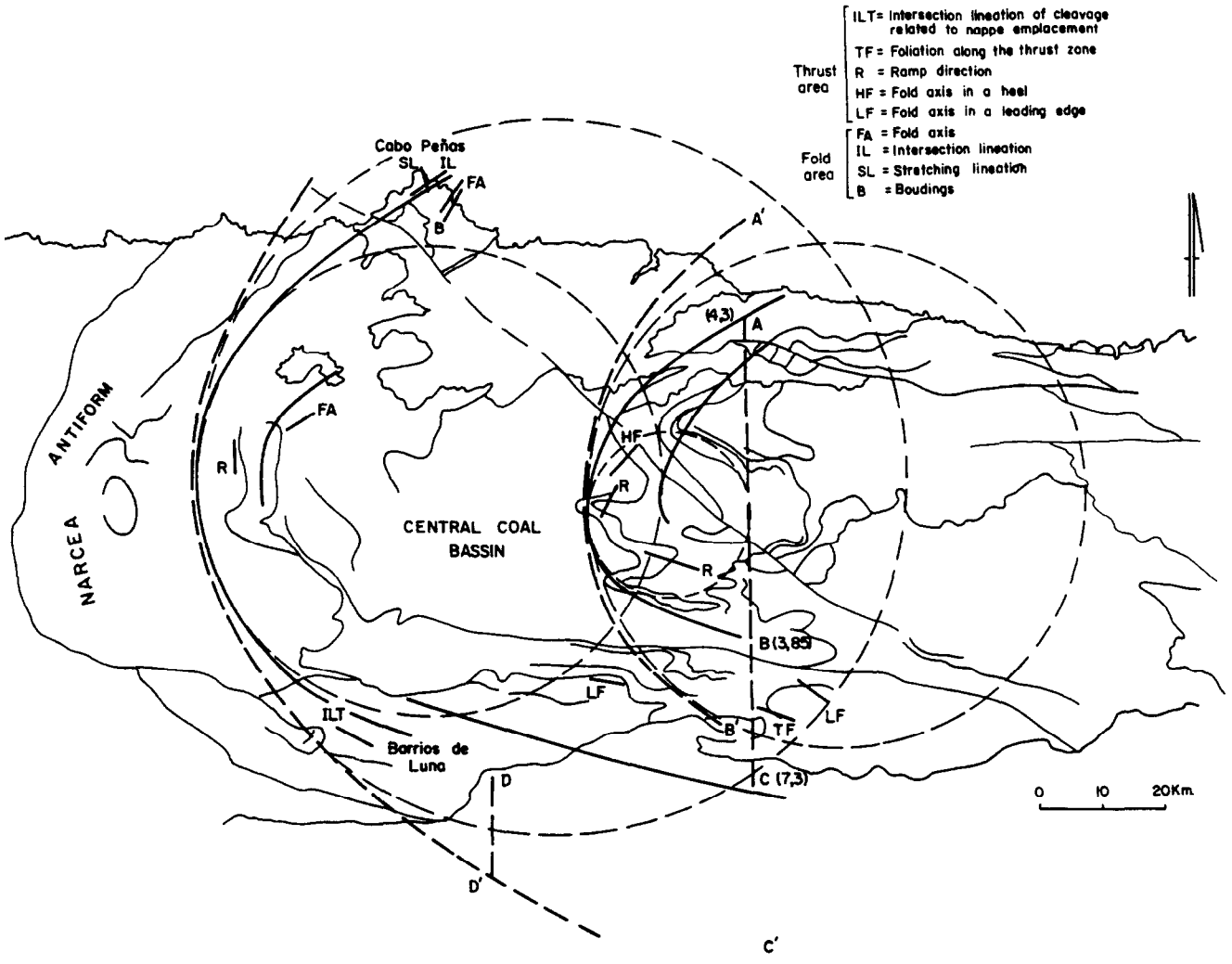

Fig. 12. Sketch of the Cantabrian zone with the available data on the direction of the first-phase structures. From these data the arc described by the first-phase structures has been drawn (full lines). The small circles show the curvature at the hinge zone of these arcs. Broken lines represent the arc after unfolding the radial set of folds and large circles the curvature of the new arc in the hinge zone.

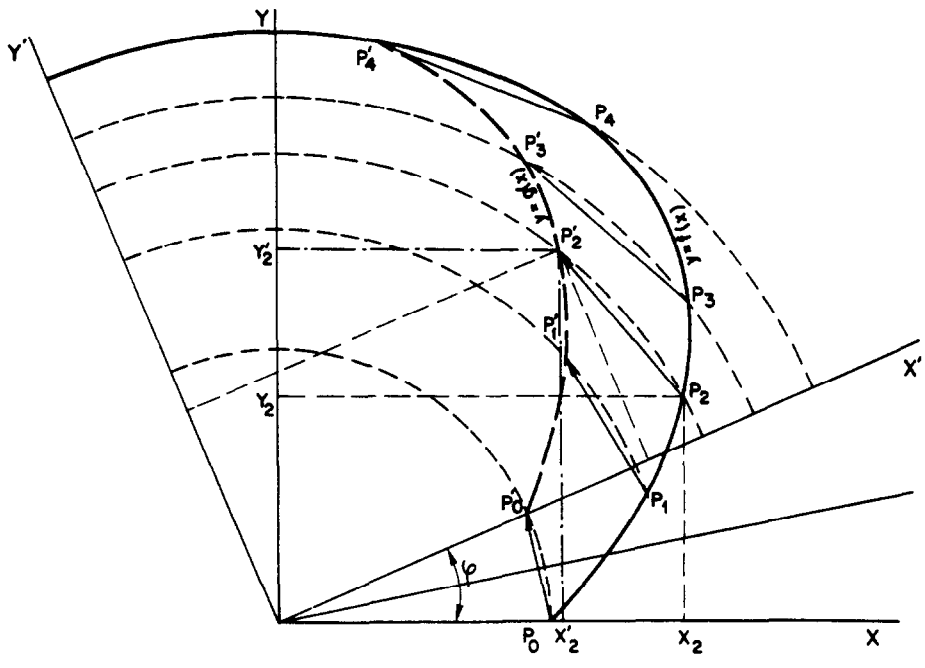

Fig. 13. Rotational emplacement of a thrust sheet with a curved trace ending (lower part) against an anticline–syncline couple.

one extreme against a fold system and at the other coincides with a strike-slip fault; (2) the slip is oblique to the trace of the overthrust; (3) the maximum overlap occurs in the 'central' part of the thrust sheet and may decrease over a short distance in both directions and (4) the curved trace gives the impression that the overlap decreases towards the frontal part of the thrust sheet.

All the above characteristics fit those of the thrust sheets in the Cantabrian zone, especially those in the Ponga nappe province.

A last problem concerns the traces of the strike-slip faults at one end of the overthrust. We recall that the Cantabrian zone is formed by an array of anastomosing thrust surfaces; thus, the strike-slip displacements must concentrate on both sides of the arc, where the displacements are probably absorbed by E–W trending strike-slip faults or shear zones, according to the model of the evolution of the arc given by Matte & Ribeiro (1975) and Julivert *et al.* (1977).

A MODEL FOR THE CANTABRIAN ZONE

A model for the Cantabrian zone can be presented, consisting of five main thrust units, some of them broken into several slices; the Somiedo–Correcilla unit, formed by five slices, the La Sobia–Bodón unit, with four slices, the Laviana and Rioseco thrust sheets, and the Ponga nappe, with many minor slices.

Each of the main units was emplaced with a rotational movement with rotation centred on the nappe termination. Each slice within the same unit moved with a certain independence, suffering additional rotations around centres located at local terminations. Each unit did not move as a rigid plate, but was being curved as it was emplaced.

In this way, the arc suffered a first tightening during nappe emplacement. The angle between NRM in the northern part of the Belmonte thrust sheet and in the Luna area that remains after unfolding the radial set of folds can be explained by the counterclockwise rotation of the different slices of the Somiedo–Correcilla unit during their emplacement.

In the nappe and fold province all centres of rotation were located at the northwestern end of the thrust sheets, but in other areas such as the Laviana thrust sheet, the rotation centre was placed to the south where the sheet dies out into a syncline–anticline couple. Thus, the relative movements of the thrust sheets are complex. With this kinematic model the formation of a curved thrust belt in which the apparent movement has been towards the central part of the arc can be explained without space problems.

As deformation progressed, the thrust sheets began to fold longitudinally. The development of the longitudinal folds deforming the nappes probably led to a tightening of the arc, but must also have generated some additional space problems. Finally, the radial fold set was formed and the arc took on the form that we see at present.

This explanation of the orogenic evolution is consistent with the interpretation given by Matte & Ribeiro (1975) and by Julivert *et al.* (1977) of a relative westwards movement of the core of the arc. This movement would produce a progressive increasing of the curvature, together with an important shortening in the direction of the axial trace of the arc and the formation of strike-slip faults in its limbs. This movement component does not explain all the structures around the arc; it must be combined with other displacements that took place simultaneously or successively during orogeny.

The relative westwards movement of the core of the arc must have produced crustal shortening in that direction (continental collision has been suggested to explain the emplacement of the catazonal massifs of Galicia and northern Portugal; Bard *et al.* 1980). The thrusts and folds in the Cantabrian zone can be best interpreted as representing cover rather than crustal shortening; probably only the sedimentary cover is affected, the whole crust only being involved in more internal parts of the chain.

Acknowledgements—The authors are grateful to J. G. Ramsay for critical reading of the manuscript and revision of the English text. Also thanks are given to two anonymous referees and to J. Soldevila who participated in some of the geological field studies. J. M. Ros drew the figures.

REFERENCES

Arboleya, M. L. 1981. La estructura del manto del Esla (Cordillera Cantábrica, León). *Bol. Geol. Min. Inst. Geol. Min. Espana* **92**, 19–40.

Bard, J. P., Burg, J. P., Matte, Ph. & Ribeiro, A. La chaîne hercynienne d'Europe occidentale en termes de tectonique des plaques. Coll. C 6 Géologie de l'Europe. 26 CGI *Mem. Bur. Rech. geol. min. Fr.* 108.

Berger, P. & Johnson, A. M. 1980. First-order analysis of deformation of a thrust sheet moving over a ramp. *Tectonophysics* **70**, T9–T24.

Blay, P., Cosgrove, J. W. & Summers, J. M. 1977. An experimental investigation of the development of structures in multilayers under the influence of gravity. *J. geol. Soc. Lond.* **133**, 329–342.

Bonhommet, N., Cobbold, P. R., Perroud, H., & Richardson, A. 1981. Paleomagnetism and cross-folding in a key area of the Asturian arc (Spain). *J. geophys. Res.* **86**, 1873–1887.

Boyer, S. E. & Elliott, D. 1982. Thrust systems. *Bull. Am. Ass. Petrol. Geol.* **66**, 1196–1230.

Butler, R. W. H. 1982. The terminology of structures in thrust belts. *J. Struct. Geol.* **4**, 239–245.

Butts, Ch. 1927. Fensters in the Cumberland overthrust block in southwestern Virginia. *Bull. geol. Surv. Virg.* **28**, 1–12.

Cloos, E. 1961. Bedding slips, wedges and folding in layered sequences. *C. r. Somm. Séanc. Soc. geol. Finlande* 33.

Elliott, D. 1976. The energy balance and deformation mechanisms of thrust sheets. *Phil. Trans. R. Soc.* **A283**, 289–312.

Gardner, D. A. C. & Spang, J. H. 1973. Model studies of the displacement transfer associated with overthrust faulting. *Bull. Can. Petrol. Geol.* **21**, 534–552.

Julivert, M. 1971a. Decollement tectonics in the Hercynian Cordillera of Northwest Spain. *Am. J. Sci.* **270**, 1–29.

Julivert, M. 1971b. L'evolution structurale de l'arc asturien. In: *Histoire Structurale du Golfe de Gascogne*. 1. Technip, Paris, **1**, 2–28.

Julivert, M. 1976. La estructura de la región del Cabo Peñas. *Trab. Geol. Univ. Oviedo* **8**, 203–309.

Julivert, M. & Marcos, A. 1973. Superimposed folding under flexural conditions in the Cantabrian zone (Hercynian Cordillera, Northwest Spain). *Am. J. Sci.* **273**, 353–375.

Julivert, M., Marcos, A. & Perez-Estaún, A. 1977. La estructure de la chaîne hercynienne dans le secteur ibérique et l'arc ibero-armoricain. In: *La Chaîne Varisque d'Europe Moyenne et Occidentale. Coll. Int. C.N.R.S.*, Rennes 1974, **243**, 429–440.

Marcos, A. & Arboleya, M. L. 1975. Evidence of progressive deformation in minor structures. *Geol. Rdsch.* **64**, 278–287.

Matte, Ph. & Ribeiro, A. 1975. Forme et orientation de l'ellipsoïde de déformation dans la virgation hercynienne de Galice. Relations avec le plissement et hypothèses sur la genese de l'arc ibero-armoricain. *C. r. hebd. Séanc. Acad. Sci., Paris* **280**, 2825–2828.

Perroud, H. & Bonhommet, N. 1981. Paleomagnetism of the Ibero-Armorican arc and the Hercynian orogeny in Western Europe. *Nature, Lond.* **292**, 445–448.

Pfiffner, O. A. 1981. Fold-and-thrust tectonics in the Helvetic Nappes (E Switzerland). In: *Thrust and Nappe Tectonics* (edited by McClay, K. R. & Price, N. J.). *Spec. Publs geol. Soc. Lond.* **9**, 319–327.

Ramsay, J. G. 1974. Development of chevron folds. *Bull. geol. Soc. Am.* **85**, 1741–1754.

Rich, J. L. 1934. Mechanics of low-angle overthrust faulting as illustrated by Cumberland thrust block, Virginia, Kentucky and Tennessee. *Bull. Am. Ass. Petrol. Geol.* **18**, 1584–1596.

Ries, A. C. & Shackleton, R. M. 1976. Patterns of strain variation in arcuate fold belts. *Phil. Trans. R. Soc.* **283A**, 281–288.

Ries, A. C., Richardson, A. & Shackleton, R. M. 1980. Rotation of the Iberian arc: palaeomagnetic results from North Spain. *Earth Planet. Sci. Lett.* **70**, 301–310.

Rodgers, J. 1963. Mechanics of Appalachian foreland folding in Pennsylvania and West Virginia. *Bull. Am. Ass. Petrol. Geol.* **47**, 1527–1536.

Suppe, J. & Namson, J. 1979. Fault-bend origin of frontal folds of the Western Taiwan fold-and-thrust belt. *Petrol. Geol. Taiwan* **16**, 1–18.

Wilson, C. W. & Stearns, R. G. 1958. Structure of the Cumberland Plateau, Tennessee. *Bull. geol. Soc. Am.* **69**, 1283–1296.

Zamarreño, I. 1972. Las litofacies carbonatadas del Cámbrico de la Zona Cantábrica (NW de España) y su distribución paleogeografica. *Trab. Geol. Univ. Oviedo* **5**, 1–118.

Zamarreño, I. 1975. Peritidal origin of Cambrian Carbonates in Northwest Spain. In: *Tidal Deposits: A Case Book of Recent Examples and Fossil Counterparts* (edited by Ginsburg, R. N.). Springer, Berlin, 323–332.